The Canadian Mineralogist
Vol. 46, pp. 219-231 (2008)
DOI: 10.3749/canmin.46.1.219

THE SULFIDES AND SELENIDES OF THE MUSONOÏ MINE, KOLWEZI, KATANGA, DEMOCRATIC REPUBLIC OF CONGO

CASSIAN PIRARD AND FRÉDÉRIC HATERT

Laboratoire de Minéralogie, Université de Liège, Bâtiment B18, B–4000 Liège, Belgium

ABSTRACT

An investigation of ore minerals from the Thrust-Slice "2400'" of the Musonoï Extension mine, Katanga, Democratic Republic of Congo, has provided new insights into the origin of copper sulfides and selenides. The early sulfides are pyrite, covellite, spionkopite, and digenite, which crystallize, with authigenic quartz, during diagenesis. Metasomatic enrichment in U and Se, which is responsible for the unusual mineralogy of the Musonoï deposit, firstly gave rise to the crystallization of Cu–Pd-bearing trogtalite and various palladium selenides (oosterboschite, verbeekite and unidentified Pd–Cu–Pt–Se phases). Subsequently, Se-rich copper minerals, berzelianite and Se-bearing carrollite formed, followed by the crystallization of Se-bearing digenite. Temperature estimates based on these assemblages indicate at least 200°C. Meteoric alteration affected these primary minerals and mainly resulted in the leaching of copper. Replacement phases are spionkopite, yarrowite, and athabascaite, which formed at temperatures below 100°C. Electron-microprobe analyses show the existence of a complete solid-solution series between high digenite and berzelianite. The variation of the *a* unit-cell parameter along this solid solution follows the equation $y = -0.3446x^3 + 0.5485x^2 - 0.0358x + 5.5758$, $R^2 = 0.96$. A similar mechanism of S-for-Se substitution accounts for the precipitation of Se-bearing spionkopite and S-bearing athabascaite. These observations provide new data on the sequence of transformation affecting copper sulfides and selenides at low-temperature, meteoric conditions.

Keywords: copper sulfides, selenides, digenite–berzelianite solid solution, Musonoï mine, Katanga, Democratic Republic of Congo.

SOMMAIRE

Une étude de la minéralisation de l'Ecaille "2400" de la mine de Musonoï Extension, Katanga, République Démocratique du Congo, a permis d'acquérir de nouvelles données concernant la genèse des sulfures et séléniures de cuivre. Les sulfures les plus précoces comprennent la pyrite, la covellite, la spionkopite et la digénite, qui cristallisent avec le quartz authigène durant la diagenèse. L'enrichissement métasomatique en U et Se, responsable de la minéralisation exceptionnelle de la mine de Musonoï, s'exprime par la cristallisation précoce de trogtalite cupro-palladifère et de séléniures de palladium (oosterboschite, verbeekite et une phase Pd–Cu–Pt–Se). Les minéraux sélénio-cuprifères sont ensuite apparus, avec la berzélianite et la carrollite sélénifère, suivis de digénite sélénifère. Les températures de ces assemblages minéralogiques sont estimées à plus 200°C. L'altération météorique a affecté ces phases primaires, provoquant une libération du cuivre en solution. Les sulfures de remplacement sont la spionkopite, la yarrowite et l'athabascaïte, qui auraient une température de formation inférieure à 100°C. Les analyses chimiques de ces minéraux à la microsonde électronique ont montré qu'il existe une solution solide complète entre la digénite de haute température et la berzélianite. La variation du paramètre cristallographique *a* le long de cette solution solide suit l'équation: $y = -0{,}3446x^3 + 0{,}5485x^2 - 0{,}0358x + 5{,}5758$, $R^2 = 0{,}96$. Un mécanisme de substitution de S à Se similaire a également été observé dans d'autres minéraux, produisant une spionkopite sélénifère et une athabascaïte sulfurée. Ces observations nous permettent de mieux appréhender les séquences de transformation des sulfures et des séléniures dans des conditions météoriques de basses températures.

Mots-clés: sulfures de cuivre, séléniures, solution solide digénite–berzélianite, mine de Musonoï, Katanga, République Démocratique du Congo.

§ *E-mail address*: fhatert@ulg.ac.be

Introduction

The Musonoï mine, known for many years as a world-class locality of uranium-, copper-, and cobalt-bearing minerals (Oosterbosch *et al.* 1964, Gauthier *et al.* 1989), is located in the western part of the Katanga Copperbelt, a few kilometers west of Kolwezi, in the Democratic Republic of Congo. This mine, and the nearby Kamoto mine, have been exploited since the beginning of the 20th century for copper and cobalt. Initially, the Musonoï mine was mined for chalcocite and digenite. These minerals are intergrown with minor carrollite, the main cobalt-bearing phase of this deposit.

In the 1950s, an orebody strongly enriched in uranium and selenium was discovered in the area of "Thrust-Slice 2400", but left unexploited. A part of this radioactive and complex Cu–U–Se-bearing ore was stockpiled, and subsequently studied by mineralogists in the 1960s, leading to the description of four new mineral species: guilleminite, $Ba(UO_2)_3(SeO_3)_2O_2{\bullet}3H_2O$ (Pierrot *et al.* 1965), demesmaekerite, $Pb_2Cu_5(UO_2)_2(SeO_3)_6(OH)_6{\bullet}2H_2O$ (Cesbron *et al.* 1965), marthozite, $Cu(UO_2)_3(SeO_3)_2O_2{\bullet}8H_2O$ (Cesbron *et al.* 1969), and derriksite, $Cu_4(UO_2)(SeO_3)_2(OH)_6$ (Cesbron *et al.* 1971). Musonoï is also the type locality for kolwezite, $(Co,Cu)_2(CO_3)(OH)_2$ (Deliens & Piret 1980), and for two palladium selenides: oosterboschite, $(Pd,Cu)_7Se_3$ (Johan *et al.* 1970), and verbeekite, $PdSe_2$ (Roberts *et al.* 2002).

Recently, we received several samples from the Musomoï mine, which allowed us to re-investigate the exotic mineralogy of this locality. The M.Sc. thesis of Pirard (2005) provided a general survey of this complex assemblage of minerals. In this paper, we focus on the sequence of transformations affecting the copper sulfides and selenides at Musonoï.

Geological Setting

The Musonoï mine has been excavated in an area called the Kolwezi klippe. This Precambrian thrust-outlier is a folded and faulted unit of the Katanguian overthrust, which occurs a few tens of kilometers further south (Fig. 1). Here, we focus on the Musonoï Extension Pit, which lies in Neoproterozoic rocks of the Roan 2 Formation (François & Cailteux 1981, François 1987) (Fig. 2), and especially on a tectonic unit a few hundred meters in length and a few tens of meters thick. This unit, named "Ecaille 2400" by local workers, consists of dolomitic sandstones strongly enriched in copper sulfides. Along with copper and cobalt minerals, this unit is also enriched in numerous exotic elements such as U, V, Se, Pb, Cr, or Mo, concentrated by metasomatic processes (Oosterbosch *et al.* 1964). The following sulfides and selenides were identified: Se-bearing digenite, Se-bearing covellite, Cu- and Pd-bearing trogtalite, oosterboschite, and verbeekite (Oosterbosch *et al.* 1964, Johan *et al.* 1970, Roberts *et al.* 2002).

Analytical Methods

Powder X-ray-diffraction patterns were recorded with a Debye–Scherrer camera 114.6 mm in diameter using Cu$K\alpha$ radiation (λ 1.5418 Å), or with a Philips PW–3710 diffractometer using Fe$K\alpha$ radiation (λ 1.9373 Å). The unit-cell parameters of members of the digenite–berzelianite series were calculated with the least-squares refinement program LCLSQ 8.4. (Burnham 1991), from the *d*-values measured on Debye–Scherrer photographs and corrected by the Straumanis method (Nuffield 1966).

Chemical analyses were performed with a CAMECA SX50 electron microprobe operating in wavelength-dispersion mode at the Ruhr-Universität Bochum, Germany. Measurement conditions were: acceleration voltage 15 kV, beam current 15 nA, beam diameter 5 μm. The counting time per element was 30 s. We used the following standards: synthetic CuS (Cu, S), pure metallic cobalt (Co), synthetic NiO (Ni), pure metallic palladium (Pd), andradite (Fe), and synthetic ZnSe (Se).

Mineralogical Descriptions

Digenite, $Cu_{1.8}S$

Digenite is the main ore mineral in "Thrust-Slice 2400". It generally occurs in crystals a few millimeters in length, as a cement between quartz grains. This mineral shows a dark grey color, is rarely euhedral, and in most cases exhibits a {111} cleavage. In polished sections, digenite is bluish white and has a good polish, with numerous visible cleavage planes. Fractures and cleavages are commonly filled by malachite, chalcomenite, and rarely guilleminite. Spionkopite + yarrowite lamellae commonly occur along cleavage planes of the digenite (Fig. 3a). It is noteworthy that Se-bearing digenite can also be associated with white trogtalite and consequently, the contrast makes digenite appear as a very bluish mineral in reflected light.

Systematic electron-microprobe analyses showed that Co, Fe, and Ni are generally present in insignificant amounts (Table 1). The S/Se value is highly variable, and most of the investigated grains have a composition of Se-bearing digenite, with a Se/(S + Se) value ranging from 0.10 to 0.40. Some crystals represent Se-free digenite, with Se contents lower than 0.02 wt.% Se. The Cu contents range from 1.70 to 1.95 atoms per formula unit (*apfu*).

Powder X-ray-diffraction data confirm the identification of digenite. The unit-cell parameters of our samples, refined in a trigonal unit-cell (Morimoto & Kullerud 1963), show significant variations, with

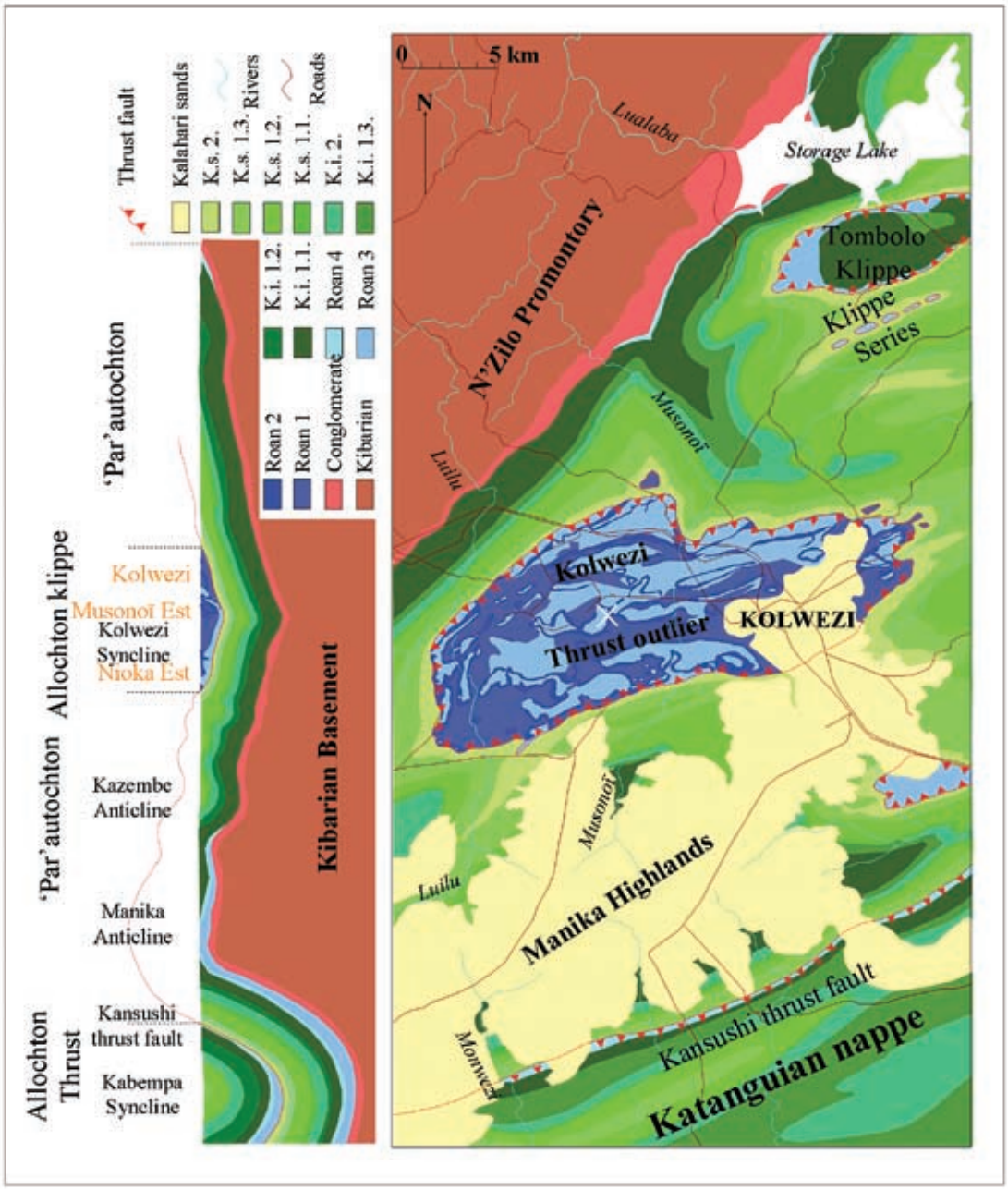

FIG. 1. Geological map of the Kolwezi area (modified from François & Cailteux 1981). The Musonoï extension mine is marked by the white cross.

3.94(1) < *a* < 4.05(2) Å and 46.1(6) < *c* < 50.5(7) Å, which can be attributed to the variations in the Se content of digenite.

Berzelianite, $Cu_{2-x}Se$

In polished sections, the crystals of berzelianite look similar to digenite, but have a better polish and less

TABLE 1. RESULTS OF ELECTRON-MICROPROBE ANALYSES OF DIGENITE AND BERZELIANITE FROM THE MUSONOÏ MINE

	Berzelianite		Digenite					
	217-5	217-20	FC7	1772	215-29	1874A	210-4	217-20
n	4	8	6	2	5	9	4	3
Cu wt.%	57.31(14)	64.58(96)	68.13(63)	70.37(62)	72.81(59)	74.53(49)	74.71(151)	79.01(9)
Co	0.02(2)	0.05(34)	0.03(2)	0.02(2)	n.d.	0.01(1)	0.02(2)	0.04(1)
Fe	0.03(3)	0.01(1)	0.02(2)	0.01(1)	0.01(2)	0.02(2)	0.03(2)	0.01(1)
Ni	0.04(3)	0.01(1)	0.02(2)	0.02(2)	n.d.	0.03(3)	0.04(3)	0.04(2)
Pd	0.03(2)	0.01(1)	0.01(2)	tr.	n.d.	0.04(4)	0.03(3)	0.01(1)
S	0.40(15)	7.24(58)	12.72(50)	14.23(11)	15.78(18)	17.69(21)	17.80(53)	20.81(27)
Se	40.40(37)	28.65(150)	19.05(88)	14.92(18)	10.78(16)	7.93(24)	5.63(99)	0.63(21)
Total	98.23(39)	100.55(40)	99.98(78)	99.57(81)	99.38(62)	100.25(58)	98.26(126)	100.55(30)
Cu *apfu*	1.72(1)	1.73(1)	1.68(1)	1.75(1)	1.82(1)	1.80(1)	1.88(5)	1.89(1)
Co	tr.	tr.	tr.	tr.	n.d.	tr.	tr.	tr.
Fe	tr.	tr.	tr.	tr.	tr.	tr.	tr.	tr.
Ni	tr.	tr.	tr.	tr.	n.d.	tr.	tr.	tr.
Pd	tr.	tr.	tr.	tr.	n.d.	tr.	tr.	tr.
S	0.02(1)	0.38(1)	0.62(2)	0.70(1)	0.78(1)	0.85(1)	0.89(1)	0.99(1)
Se	0.98(1)	0.62(1)	0.38(2)	0.30(1)	0.22(1)	0.15(1)	0.11(1)	0.01(1)

Analyst: H.J. Bernhardt. The number of point analyses *n* is indicated, standard deviations are given in parentheses. Cation numbers were calculated on the basis of one atom of sulfur + selenium per formula unit.

TABLE 2. RESULTS OF ELECTRON-MICROPROBE ANALYSES OF ATHABASCAITE, YARROWITE, AND SPIONKOPITE FROM THE MUSONOÏ MINE

	Athabascaite		Spi	Yar	Spi + Yar
	217-20	FC15	2917	FC13	1778
n	4	6	7	6	6
Cu wt.%	57.35(7)	61.04(88)	65.39(98)	63.92(37)	65.85(32)
Co	0.02(2)	0.03(2)	0.02(1)	0.01(1)	0.01(1)
Fe	0.04(6)	0.00(1)	0.02(2)	0.01(1)	0.02(2)
Ni	0.02(1)	0.02(2)	0.01(1)	0.02(1)	0.04(4)
Pd	0.02(3)	0.07(3)	0.04(5)	0.04(3)	0.06(4)
S	8.93(66)	9.82(17)	19.00(30)	19.83(38)	21.70(20)
Se	34.37(112)	30.69(52)	16.46(27)	16.82(10)	12.48(9)
Total	100.75(46)	101.67(38)	100.94(134)	100.65(64)	100.16(37)
Cu *apfu*	5.059(114)	5.53(16)	1.29(2)	1.21(2)	1.24(2)
Co	tr.	tr.	tr.	tr.	tr.
Fe	tr.	tr.	tr.	tr.	tr.
Ni	tr.	tr.	tr.	tr.	tr.
Pd	tr.	tr.	tr.	tr.	tr.
S	1.56(10)	1.76(2)	0.74(1)	0.74(1)	0.81(1)
Se	2.44(10)	2.23(2)	0.26(1)	0.26(1)	0.19(1)
Σcations/(S+Se)	1.27(3)	1.38(4)	1.29(2)	1.21(2)	1.24(2)
Se/(S+Se)	0.61(2)	0.56(1)	0.26(1)	0.26(1)	0.19(1)

Analyst: H.J. Bernhardt. The number of point analyses *n* is indicated; standard deviations are given in parentheses. Cation numbers were calculated on the basis of 4 (athabascaite) or 1 (spionkopite, yarrowite) atoms of sulfur + selenium per formula unit. Symbols: Spi: spionkopite, Yar: yarrowite.

clearly visible cleavage planes. The most selenium-rich samples from Musonoï show a greenish blue hue and a euhedral morphology (Fig. 3b). The composition of berzelianite ranges in Se/(S + Se) from 0.51 to 0.99 (Table 1).

Yarrowite, $Cu_{1.2}S$ and spionkopite, $Cu_{1.32}S$

Intergrowths of spionkopite and yarrowite occur in Se-bearing digenite, as laths several millimeters in length and of 100–300 μm wide (Fig. 3a). Colors are different from those of typical yarrowite and spionkopite, with more yellowish to creamy hues (Fig. 3c). No powder X-ray-diffraction pattern has been obtained on these minerals, because they cannot be efficiently separated from Se-bearing digenite. Electron-microprobe analyses show that our grains have a higher selenium content than those analyzed by Oosterbosch *et al.* (1964) (Table 2), with Se/(S + Se) from 0.19 to 0.30. Cobalt, Ni, and Fe were detected in very small amounts only. According to the copper contents, ranging from 1.21 to 1.29 *apfu*, the chemical compositions are well in the accepted range for yarrowite and spionkopite (Table 2). A submicroscopic intergrowth of these two minerals could give an intermediate value, with 1.24 Cu *apfu*, as previously suggested by Goble & Smith (1973) and Goble (1980).

Athabascaite, Cu_5Se_4

Among the laths of Se-bearing spionkopite + yarrowite, the Se content is in some cases greater than the S content, and the material can be considered as a copper selenide with a Se/(S + Se) value close to 0.60

(Table 2). No mineral species has yet been described as a selenium end-member of a solid solution with spionkopite or yarrowite. However, according to Picot & Johan (1982), athabascaite from Martin Lake, Saskatchewan (Harris *et al*. 1969), is close to Se-bearing spionkopite + yarrowite in term of optical properties. These authors did not know of any intermediate compound of these series, but supposed that if it exists, its reflectance characteristics would be between those of Se-bearing yarrowite + spionkopite and S-bearing athabascaite. This is exactly what is observed at Musonoï, for extremely S-rich athabascaite (Fig. 3c). The identification is confirmed by the electron-microprobe analysis (Table 2), which shows a composition $Cu_{1.27}(Se_{0.61}S_{0.39})_{\Sigma 1.00}$, close, in terms of Cu/(S + Se), to the composition $Cu_{1.276}(Se_{0.87}S_{0.13})_{\Sigma 1.00}$ of athabascaite from Martin Lake, Saskatchewan (Harris *et al*. 1969).

Trogtalite, $CoSe_2$

Trogtalite occurs as white to yellowish creamy grains in malachite, chalcomenite, or cobaltomenite, in some cases intergrown with Se-bearing digenite and berzelianite (Figs. 3d, e). The crystals are not euhedral, but mostly show a globular shape in copper sulfide veins (Fig. 3d). The electron-microprobe analyses (Table 3) show that trogtalite from Musonoï contains significant amounts of Cu (0.26 to 0.32 *apfu*) and Pd (0.06 to 0.13 *apfu*). A grain particularly enriched in palladium shows a composition $(Co_{0.55}Cu_{0.32}Pd_{0.13}Ni_{0.01}Fe_{0.01})_{\Sigma 1.03}Se_{1.94}S_{0.06}$. Trogtalite was previously described at Musonoï by Johan *et al*. (1970), who reported the chemical composition $(Co_{0.65}Cu_{0.38}Pd_{0.03})_{\Sigma 1.06}Se_2$.

Copper, Cu

Metallic Cu occurs as grains <15 μm long, closely associated with trogtalite, cobaltomenite and chalcomenite. A single-point electron-microprobe analysis confirms the identification and shows the presence of 0.14 wt.% Se.

Gold, Au

Gold is common at Musonoï; it forms homogeneous grains less than one millimeter in diameter. EDX spectra suggest only very small amounts of copper and selenium. No silver was detected. In sample FC15, gold is associated with heterogeneous, light greyish grains representing inclusions of Pd-bearing minerals.

Palladium selenides

Associated with the grains of gold are grey anhedral crystals with minute white inclusions with a stronger reflectance, less than 100 μm in diameter (Fig. 3f). The brighter phase is a primary mineral, and the greyish surrounding mineral is a product of alteration. Electron-microprobe analyses were not possible owing to the small size of these inclusions. However, energy-dispersion spectra (EDX) show that the white grains have a Pd–Cu–Pt–Se composition, which would correspond to a selenide of Pd. The grey grains seem to be more oxidized and could be a submicroscopic mixture of (Pd,Cu,Pt) selenides and oxides known as "palladinite" (PdO) (Jedwab *et al*. 1993) (Table 4). Such oxidation products have already been observed associated with palladseite ($Pd_{17}Se_{15}$) in Minas Gerais (Cabral *et al*. 2002).

Discussion

The digenite – berzelianite solid-solution series

One of the main features of the Musonoï deposit is the presence of an almost complete range of compositions between sulfides and selenides (Fig. 4). With chemical compositions from $Cu_{1.90}S_{0.99}Se_{0.01}$ to $Cu_{1.73}Se_{0.99}S_{0.01}$, the solid solution between digenite and berzelianite is well established, with only small gaps between 45 and 50% and between 70 and 95%.

TABLE 3. RESULTS OF ELECTRON-MICROPROBE ANALYSES OF TROGTALITE FROM THE MUSONOÏ MINE

n	FC15 6	FC15a 8	FC7 6	217-20 2	FC15 5
Cu wt.%	7.69(50)	7.67(18)	8.01(38)	8.85(25)	9.12(8)
Co	18.52(63)	18.63(16)	17.74(68)	16.29(97)	14.72(11)
Fe	0.14(3)	-	0.13(3)	0.17(2)	0.17(3)
Ni	0.34(4)	0.30(4)	0.33(5)	0.34(2)	0.38(8)
Pd	3.02(39)	2.92(27)	3.63(38)	4.88(93)	6.20(19)
S	1.19(8)	1.30(5)	1.10(3)	1.04(16)	0.86(4)
Se	70.23(25)	70.21(18)	70.17(26)	69.67(5)	69.43(15)
Total	101.13(22)	101.03(38)	101.11(49)	101.24(5)	100.88(17)
Cu *apfu*	0.26(2)	0.26(1)	0.27(1)	0.30(1)	0.32(1)
Co	0.69(1)	0.68(1)	0.65(2)	0.63(4)	0.55(1)
Fe	0.01(1)	-	0.01(1)	0.01(1)	0.01(1)
Ni	0.01(1)	0.01(1)	0.01(1)	0.01(1)	0.01(1)
Pd	0.06(1)	0.06(1)	0.07(1)	0.10(2)	0.13(1)
S	0.08(1)	0.09(1)	0.07(1)	0.07(1)	0.06(1)
Se	1.92(1)	1.91(1)	1.93(1)	1.93(1)	1.94(1)
Σcations	1.03(2)	1.01(1)	1.02(1)	1.05(1)	1.02(1)

Analyst: H.J. Bernhardt. The number of point analyses *n* is indicated, and standard deviations are given in parentheses. Cation numbers were calculated on the basis of two atoms of sulfur + selenium per formula unit.

TABLE 4. PEAK INTENSITY IN THE ENERGY-DISPERSION SPECTRA (EDX) OF PALLADIUM-BEARING PHASES FROM THE MUSONOI MINE

	Pd*L*α	Pt*L*α	Se*K*α	Cu*K*α	O*K*α	Background
Low-brightness BSE	9.1	1.2	3.3	3.7	6.0	0.6 to 0.1
High-brightness BSE	9.0	0.7	3.8	0.4	0.3	0.6 to 0.1

Analyst: H.J. Bernhardt. Values are given in counts per second over 100 seconds.

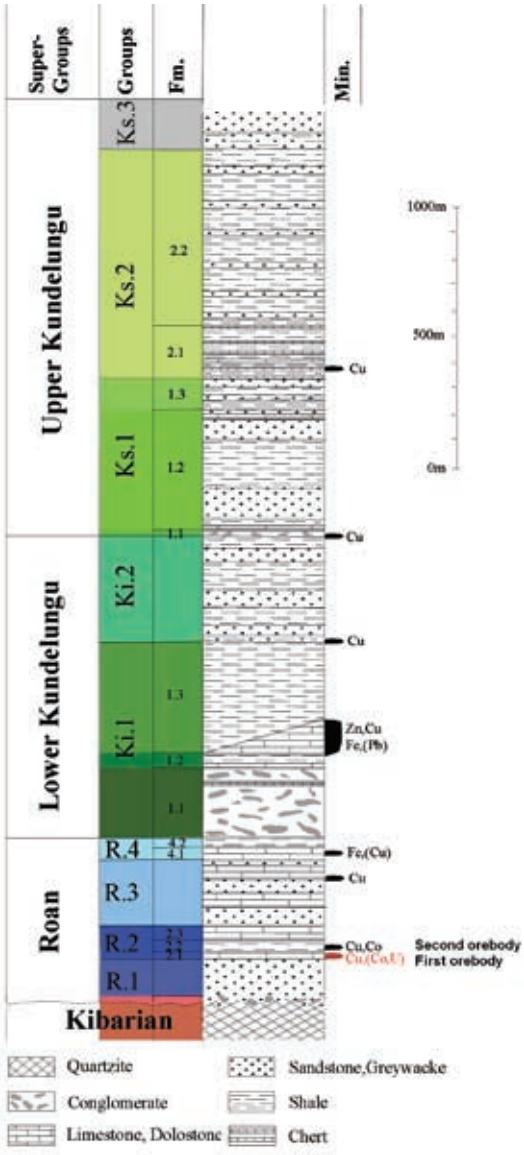

FIG. 2. Lithological scale of Katanguian overthrust in the Kolwezi area (modified from François 1993).

These chemical results were coupled with powder X-ray-diffraction data for 12 samples, 11 of Se-bearing digenite with Se/(S + Se) values from 0.14 to 0.40, and one of S-bearing berzelianite with a Se/(S + Se) value of 0.63. Berzelianite displays a cubic symmetry, *Fm*3*m*, with *a* equal to 5.694(7) Å (Earley 1950), whereas low digenite is trigonal, $R\bar{3}m$, *a* 3.92, *c* 48.0 Å (Donnay *et al.* 1958). However, in order to allow the comparison of the unit-cell parameters of digenite with that of berzelianite, the indexation of the cubic high-temperature form of digenite has been chosen.

The data show a correlation between the Se content and the crystallographic parameters (Fig. 5, Table 5), with unit-cell dimension increasing from 5.57 Å to 5.75 Å with increasing selenium content. The regression curve obtained is not linear and cannot therefore be fitted with Vegard's law (Zen 1956). The most convenient fit for this scatter is a third-order polynomial curve: $y = -0.3446x^3 + 0.5485x^2 - 0.0358x + 5.5758$, with $R^2 = 0.96$. Because Vegard's law only applies to cubic compounds, the observed non-linear behavior could be partly explained by the trigonal symmetry of low digenite. Moreover, despite the fact that the crystal structure of natural berzelianite has never been described, Yamamoto & Kashida (1991) suggested that the low-temperature structure of synthetic copper selenide could be similar to the structure of low digenite. As this type of trigonal Cu_2Se has never been observed in nature, we prefer to use the cubic setting, which has been reported for both digenite and berzelianite. In addition, selenium in the digenite structure could stabilize

TABLE 5. THE UNIT-CELL PARAMETER *a* IN THE DIGENITE–BERZELIANITE SOLID-SOLUTION SERIES

Locality	Chemical composition	Se/(S + Se)	a (Å)
	Harris *et al.* (1970)		
Martin Lake	$Cu_{1.751}Se_{1.000}$	1.00	5.740(1)
Synthetic	$Cu_{1.801}Se_{1.000}$	1.00	5.746(1)
Western Moravia	$Cu_{1.854}Se_{1.000}$	1.00	5.748(2)
Synthetic	$Cu_{1.806}Se_{0.826}S_{0.173}$	0.826	5.724(2)
Synthetic	$Cu_{1.790}Se_{0.699}S_{0.300}$	0.699	5.702(1)
Synthetic	$Cu_{1.686}Se_{0.499}S_{0.501}$	0.499	5.653(2)
Martin Lake	$Cu_{1.797}Se_{0.683}S_{0.317}$	0.683	5.696(3)
	Morimoto & Kullerud (1963)		
Synthetic	$Cu_{1.800}S_{1.000}$	0.00	5.570(5)
	Earley (1950)		
Skrikerum	$Cu_{2-x}Se_{1.000}$	1.00	5.739
	Oosterbosch *et al.* (1964)		
Musonoï	$Cu_{1.78}Se_{0.36}S_{0.64}$	0.36	5.62
	This study		
210-4	$Cu_{1.816}Se_{0.150}S_{0.850}$	0.150(7)	5.586(9)
211-16	$Cu_{1.782}Se_{0.156}S_{0.844}$	0.156(5)	5.586(12)
215-20	$Cu_{1.774}Se_{0.187}S_{0.813}$	0.187(13)	5.590(4)
215-11	$Cu_{1.725}Se_{0.214}S_{0.786}$	0.214(11)	5.584(15)
215-29	$Cu_{1.822}Se_{0.217}S_{0.783}$	0.217(4)	5.599(9)
214-3	$Cu_{1.750}Se_{0.218}S_{0.782}$	0.218(4)	5.580(12)
FC13	$Cu_{1.672}Se_{0.257}S_{0.743}$	0.257(4)	5.595(9)
211-12	$Cu_{1.752}Se_{0.266}S_{0.734}$	0.266(4)	5.604(7)
214-19	$Cu_{1.724}Se_{0.282}S_{0.718}$	0.282(4)	5.587(16)
211-7	$Cu_{1.746}Se_{0.299}S_{0.701}$	0.299(3)	5.610(10)
211-18	$Cu_{1.720}Se_{0.308}S_{0.692}$	0.308(3)	5.613(15)
217-5	$Cu_{1.718}Se_{0.362}S_{0.638}$	0.362(11)	5.609(14)
FC7	$Cu_{1.757}Se_{0.375}S_{0.625}$	0.375(15)	5.623(11)
217-20	$Cu_{1.718}Se_{0.625}S_{0.375}$	0.625(28)	5.690(9)

Chemical compositions are calculated on the basis of one atom of sulfur + selenium per formula unit. Unit-cell parameters are calculated on the basis of high-digenite structure. All literature data have been measured by X-ray powder diffraction.

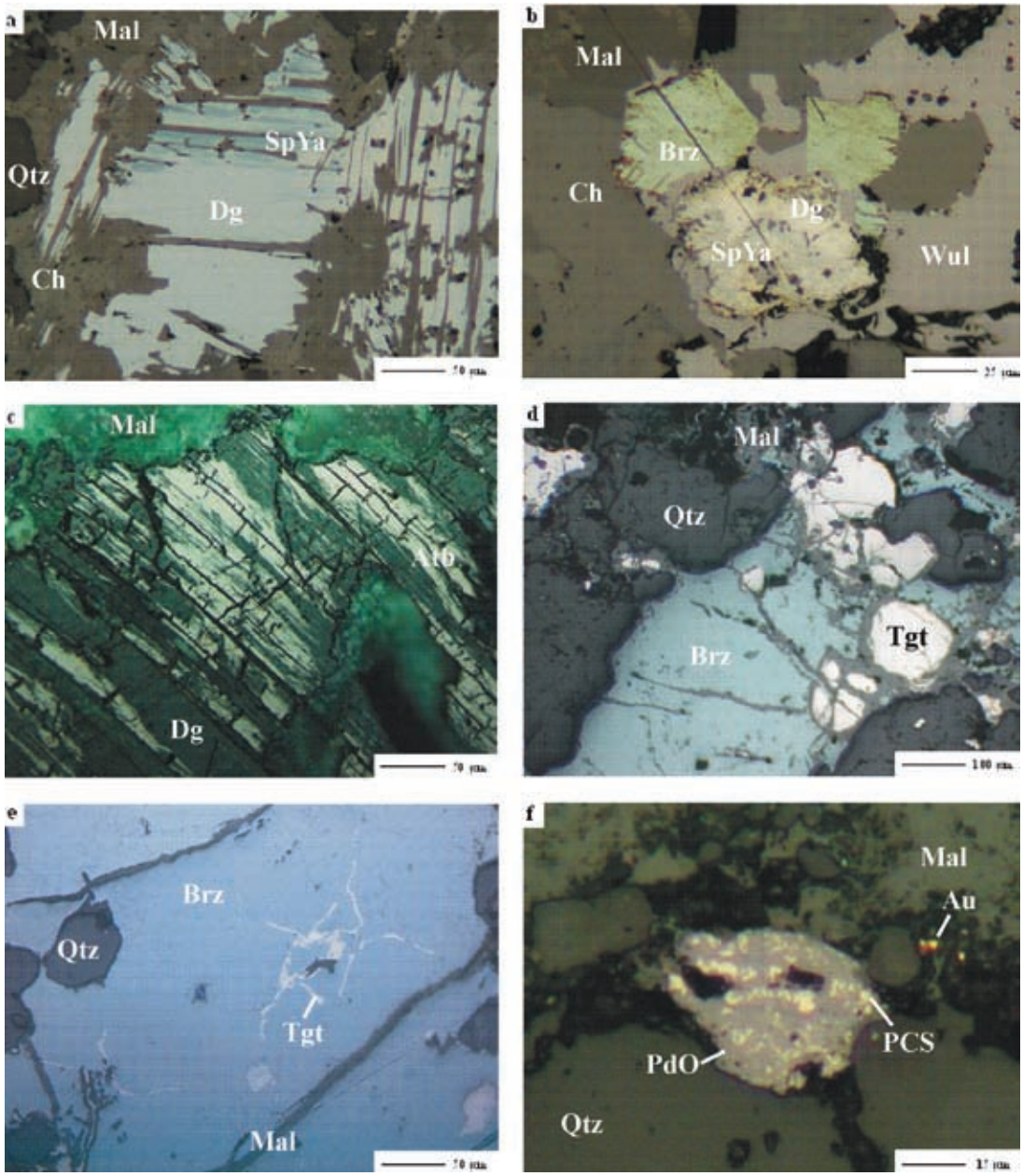

FIG. 3. a. Replacement of Se-bearing digenite (Dg) by lamellar Se-bearing spionkopite + yarrowite (SpYa). These sulfides are altered to malachite (Mal) and chalcomenite (Ch), which occur between quartz grains (Qtz). Reflected light, plane-polarized light (sample 1778). b. Grains of euhedral berzelianite (Brz) with Se-bearing digenite (Dg) altered by Se-bearing spionkopite + yarrowite (SpYa). Sulfides are partly replaced by wulfenite (Wul) (Pirard 2005) and by malachite (Mal) and chalcomenite (Ch). Reflected light, plane-polarized light (sample 217–5). c. Replacement of Se-bearing digenite (Dg) by S-bearing athabascaite lamellae (Atb). Sulfides grains are surrounded by malachite (Mal) vugs. Reflected light, crossed polars (sample 2917). d. Grains of anhedral trogtalite (Tgt) partly replaced by a veinlet of sulfur-bearing berzelianite (Brz) in malachite-cemented (Mal) quartz (Qtz). Reflected light, plane-polarized light (sample 217–20). e. Symplectitic intergrowth of Cu–Pd-bearing trogtalite (Tgt) in sulfur-bearing berzelianite (Brz). Quartz grains (Qtz) and malachite veins (Mal) also occur. Reflected light, plane-polarized light (sample 217–20). f. Palladium–copper selenide grains (PCS) replaced by palladium oxide (PdO) with some gold (Au) in quartz (Qtz) and malachite (Mal). Reflected light, plane-polarized light (sample FC15).

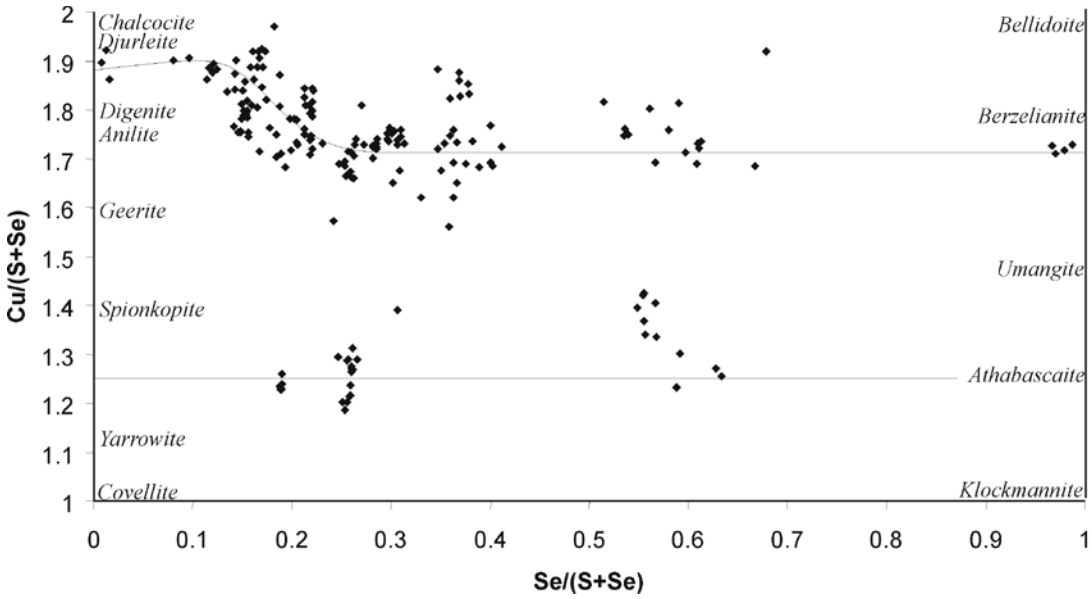

FIG. 4. Variations in chemical composition of copper sulfides and selenides from the Musonoï mine.

the cubic symmetry of high digenite at room temperature. In this case, considering the digenite–berzelianite series as a cubic solid-solution series is realistic.

The spionkopite + yarrowite – athabascaite relationship

As seen in Figure 4 and Table 2, intermediate compositions may exist between athabascaite and spionkopite + yarrowite. According to ore microscopic observations, optical features such as bireflectance and anistropism are very similar to those of Se-bearing covellite described by Picot & Johan (1982), and also to those of the hypothetical S-bearing athabascaite. Electron-microprobe analyses show that these selenium-bearing yarrowite + spionkopite have a Cu/(S + Se) value close to 1.25 (Fig. 4, Table 2). Such an intermediate composition could be interpreted as a submicroscopic intergrowth of yarrowite and spionkopite, as already suggested by Goble & Smith (1973), who noticed a statistical abundance of samples with this composition. This value of Cu/(S + Se) is similar to that in athabascaite, thus indicating that the athabascaite solid-solution could extend far beyond the 50% replacement by sulfur.

Petrogenetic interpretations

Our chemical data and petrographic observations shed light on the genesis of the Musonoï ore (Fig. 6). After deposition of the host rock, formed mainly of quartz and dolomite, an early stage of diagenesis occurred, with the crystallization of some copper- and iron-bearing sulfides such as pyrite, digenite, spionkopite + yarrowite, and covellite. Euhedral crystals of Cu-rich pyrite and iron-bearing copper sulfides occur as inclusions and are obviously contemporaneous or earlier than the authigenic crystals of quartz.

The selenium content of sulfides increased significantly at the beginning of metasomatic processes (Fig. 6). According to the morphology of grains of trogtalite [$CoSe_2$], which are globular owing to later reactions (Fig. 3d), it seems that it is one of the first important ore minerals to crystallize. Uranium deposition is strongly linked with selenium enrichment (Lambert *et al*. 2001), and uraninite veins cut by boreholes below the oxidation zone (Oosterbosch *et al*. 1964) could be related to these early processes of enrichment. The Co–U–Se-bearing fluid, from which the cobalt selenide deposited, also seems to have been enriched in platinum-group elements. This is illustrated by the strong Pd content of trogtalite and the crystallization of minerals such as verbeekite [$PdSe_2$], oosterboschite [$(Pd,Cu)_7Se_5$] (Johan *et al*. 1970, Roberts *et al*. 2002), and undetermined palladium minerals. The next stage of crystallization involved a fluid richer in copper than in cobalt. Selenium-bearing carrollite [$CuCo_2(S,Se)_4$] (Jedwab 1997, Dewaele *et al*. 2006) and crystals of Co-bearing berzelianite [$(Cu,Co)_{2-x}Se_2$] characterize this transition by including symplectitic intergrowths of Cu-bearing trogtalite [$(Co,Cu)Se_2$] (Fig. 3e).

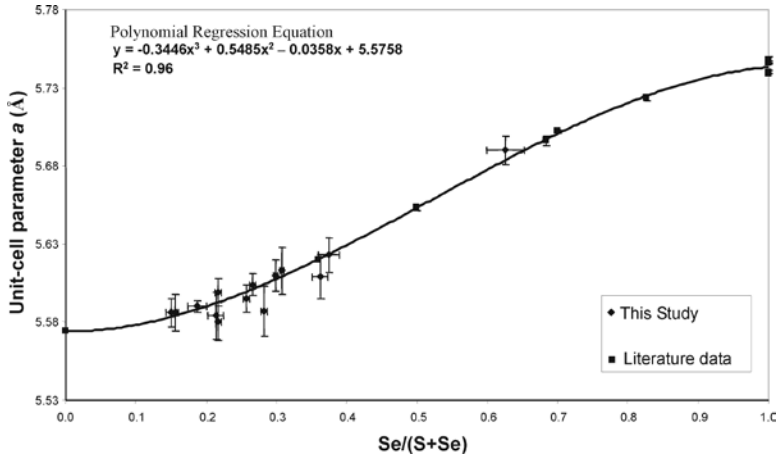

FIG. 5. Increasing *a* unit-cell parameter in digenite–berzelianite solid-solution series as Se/(S + Se) increases.

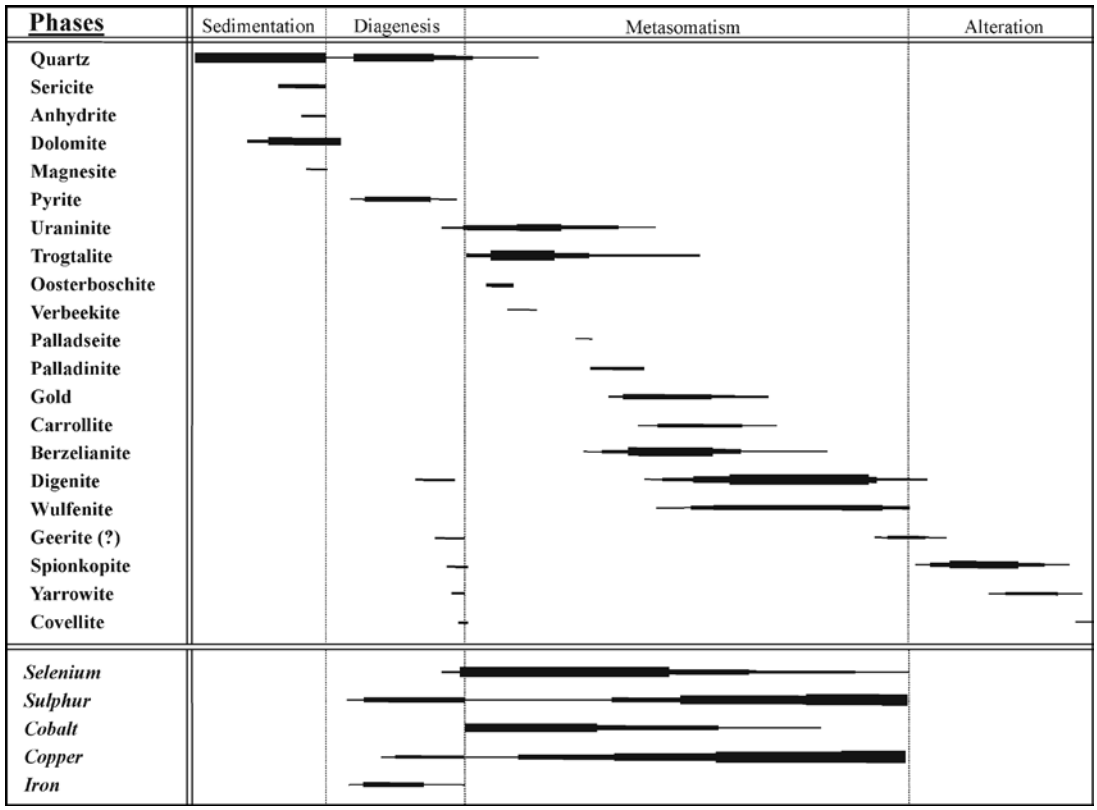

FIG. 6. Evolution of parageneses and main elements during the mineralization of Musonoï ore deposit (Oosterbosch *et al*. 1964, Johan *et al*. 1970, Jedwab 1997, Roberts *et al*. 2002, Pirard 2005, Dewaele *et al*. 2006).

Subsequently, the level of cobalt fell in the brines, such that only pure copper minerals appeared, though still rich in selenium. These are berzelianite [$Cu_{2-x}Se$] and Se-bearing digenite [$Cu_{1.8}(S,Se)$]. Finally, pure digenite [$Cu_{1.8}S$], djurleite [$Cu_{31}S_{16}$] and chalcocite [Cu_2S] crystallized. Starting from these parageneses, the Cu–S and Cu–Se phase diagrams allow us to estimate a temperature of crystallization. The Cu–Se diagram

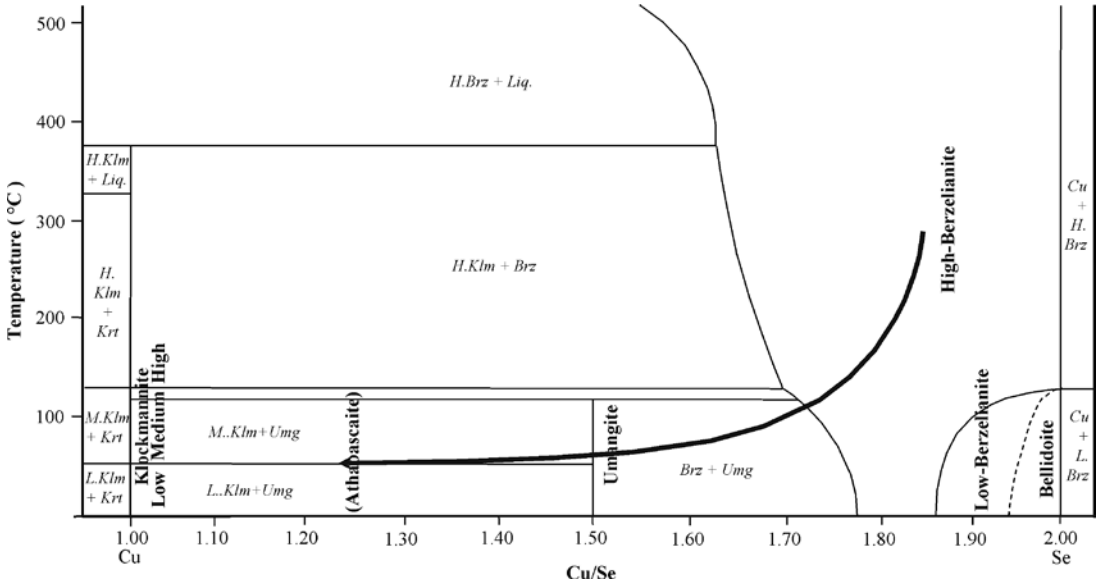

FIG. 7. Sequence of copper leaching and temperature determination on the basis of the Cu–Se phase diagram. Krt: krutaite, Klm: klockmannite, Umg: umangite, Brz: berzelianite (modified from Bernardini & Catani 1968, Chakrabarti & Laughlin 1981).

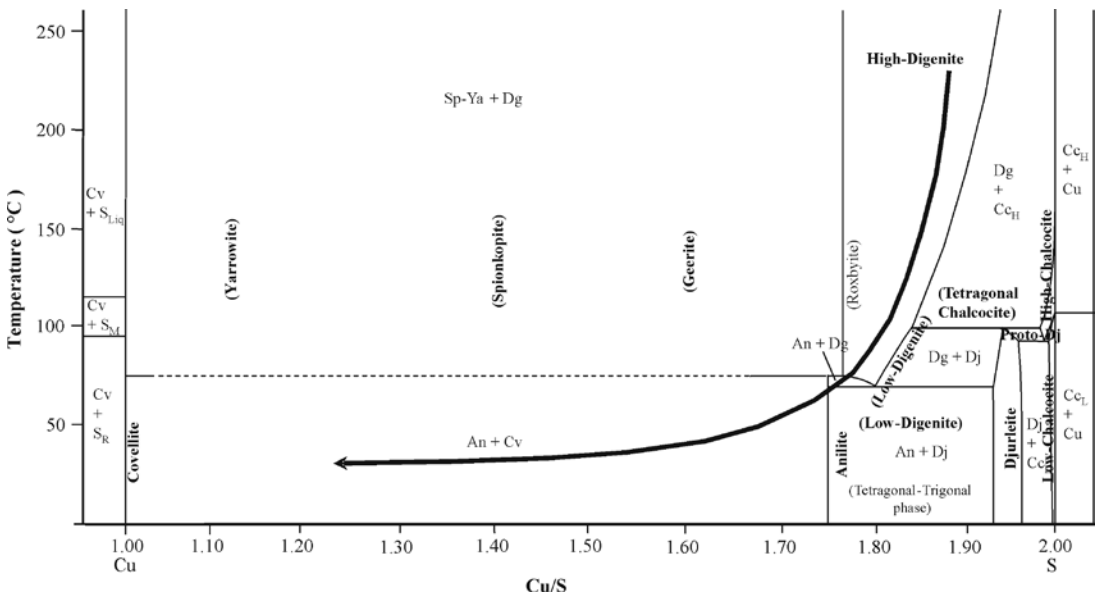

FIG. 8. Sequence of copper leaching and temperature determination on the basis of the Cu–S phase diagram. S: sulfur, Cv: covellite, Sp–Ya: spionkopite + yarrowite, An: anilite, Dg: digenite, Dj: djurleite, Cc: chalcocite (modified from Potter 1977).

(Chakrabarti & Laughlin 1981, Bernardini & Catani 1968) (Fig. 7) shows that berzelianite is not stable below 123°C, without the presence of bellidoite [Cu_2Se]. In the Cu–S diagram (Potter 1977) (Fig. 8), the composition of digenite observed at Musonoï crystallizes above 200°C in the high digenite form. These temperatures are similar to those calculated from fluid-inclusion data on authigenic quartz from Musonoï, which are 80–195°C (Dewaele *et al*. 2006). Equivalent measurements were obtained at Kamoto Principal by Audeoud (1982) on dolomite (230–360°C, 1.25 kbar) and by Bartholomé (1962) on Cu–Fe sulfides parageneses (200°C).

The last sequence of sulfides formed during oxidation and hydration of the deposit, probably under the influence of meteoric fluids. The obvious result of this stage is the leaching of copper from the sulfides and selenides. The evolution of these minerals through phase diagrams is shown by the curved arrows in Figures 7 and 8. The leaching of copper from digenite leads to the replacement of this phase by spionkopite + yarrowite, which crystallize at a temperature below 157 ± 3°C in the Se-free system (Moh 1964).

On the basis of the chemical data provided, two main facts must be pointed out in this alteration process. Firstly, transformation sequences are remarkably constant, with a succession Cu-rich digenite, Cu-poor digenite, and spionkopite + yarrowite. Such a leaching of copper can be experimentally reproduced (Whiteside & Goble 1986) and was recently observed in a natural environment such as the Stavelot Massif, Belgium (Hatert 2005). Another interesting feature is the stability of S/Se during the entire process of alteration. As shown in Figure 9 by vertical arrows, each sample retains a constant S/Se value in the alteration phases, from

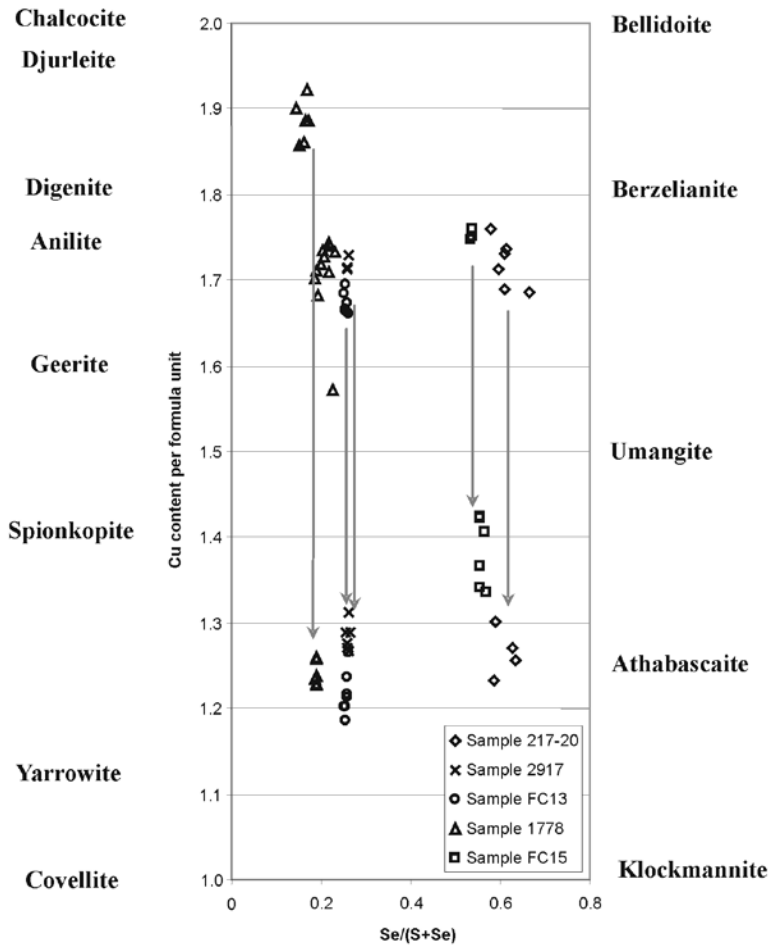

FIG. 9. Sequence of transformations as a result of copper leaching in sulfides and selenides from the Musonoï mine.

the former Se-bearing digenite to covellite. Sulfurian selenides give a similar pattern of meteoric alteration from berzelianite to athabascaite (Fig. 9). According to Harris *et al*. (1970), athabascaite is stable below 100°C and decomposes into umangite + klockmannite at higher temperature, confirming the low-temperature conditions of formation for these alteration minerals.

Acknowledgements

The authors thank A.-M. Fransolet, W. Paar, R.F. Martin, H.-J. Förster, and C.J. Stanley for their constructive comments, as well as H.J. Bernhardt for making the electron-microprobe analyses. Many thanks are due to P. du Ry and F. Coune for providing wonderful samples from the locality. The second author (F.H.) thanks the F.N.R.S. (Belgium) for a position of "Chercheur Qualifié".

References

Audeoud, D. (1982): *Les minéralisations uranifères et leur environnement à Kamoto, Kambove et Shinkolobwe (Shaba, Zaïre): pétrographie, géochimie et inclusions fluides*. Thèse, CREGU, Nancy, France.

Bartholomé, P. (1962): Les minerais cuprocobaltifères de Kamoto (Katanga Ouest). I. Pétrographie. *Studia Universitatis Lovanium, Facultés des Sciences* **14**, 3-40.

Bernardini, G.P. & Catani, A. (1968): The Cu–Se system. *Mineral. Deposita* **3**, 375-380.

Burnham, C.W. (1991): lclsq Version 8.4, Least-Squares Refinement of Crystallographic Lattice Parameters. Department of Earth & Planetary Sciences, Harvard University, Cambridge, Massachusetts.

Cabral, A.R., Lehmann, B., Kwitko, R., Galbiatti, H.F. & Pereira, M.C. (2002): Palladseite and its oxidation: evidence from Au–Pd vein-type mineralization (jacutinga), Cauê iron-ore mine, Quadrilátero Ferrífero, Minas Gerais, Brazil. *Mineral. Mag.* **66**, 327-336.

Cesbron, F., Bachet, B. & Oosterbosch, R. (1965): La demesmaekerite, sélénite hydraté d'uranium, cuivre et plomb. *Bull. Soc. fr. Minéral. Cristallogr.* **88**, 422-425.

Cesbron, F., Oosterbosch, R. & Pierrot, R. (1969): Une nouvelle espèce minérale: la marthozite. Uranyl-sélénite de cuivre hydraté. *Bull. Soc. fr. Minéral. Cristallogr.* **92**, 278-283.

Cesbron, F., Pierrot, R. & Verbeek, T. (1971): La derriksite, $Cu_4(UO_2)(SeO_3)_2(OH)_6 \bullet H_2O$, une nouvelle espèce minérale. *Bull. Soc. fr. Minéral. Cristallogr.* **94**, 534-537.

Chakrabarti, D.J. & Laughlin, D.E. (1981): The Cu–Se (copper–selenium) system: *Bull. Alloy Phase Diagr.* **2**, 305-315.

Deliens, M. & Piret, P. (1980): La kolwezite, un hydroxycarbonate de cuivre et de cobalt analogue à la glaukosphaerite et à la rosasite. *Bull. Soc. fr. Minéral. Cristallogr.* **103**, 179-184.

Dewaele, S., Muchez, P., Vets, J., Fernandez-Alonso, M. & Tack, L. (2006): Multiphase origin of the Cu–Co ore deposits in the western part of the Lufilian fold-and-thrust belt, Katanga (Democratic Republic of Congo). *J. Afr. Earth Sci.* **46**, 455-469.

Donnay, G., Donnay, J.D.H. & Kullerud, G. (1958): Crystal and twin structure of digenite, Cu_9S_5. *Am. Mineral.* **43**, 228-242.

Earley, J.W. (1950): Description and synthesis of the selenide minerals. *Am. Mineral.* **35**, 337-364.

François, A. (1987): Synthèse géologique sur l'Arc cuprifère du Shaba (Rep. du Zaïre). *Bull. Soc. belge Géol., Centenaire 1987, Hors série*, 15-65.

François, A. (1993): La structure tectonique du katanguien dans la région de Kolwezi (Shaba, Rep. du Zaïre). *Ann. Soc. Géol. Belgique* **116**, 87-104.

François, A. & Cailteux, J. (1981): La couverture katangienne entre les socles de Zilo et de la Kabompo, République du Zaïre – Région de Kolwezi. *Ann. Musée Royal Afrique Centrale, sér.* 8, *Sci. Géol.* **87**.

Gauthier, G., François, A., Deliens, M. & Piret, P. (1989): The uranium deposits of the Shaba region, Zaïre. *Mineral. Rec.* **20**, 265-304.

Goble, R.J. (1980): Copper sulfides from Alberta: yarrowite Cu_9S_8 and spionkopite $Cu_{39}S_{28}$. *Can. Mineral.* **18**, 511-518.

Goble, R.J. & Smith, D.G. (1973): Electron microprobe investigation of copper sulphides in the Precambrian Lewis series of S.W. Alberta, Canada. *Can. Mineral.* **12**, 95-103.

Harris, D.C., Cabri, L.J. & Kaiman, S. (1969): Athabascaite: a new copper selenide mineral from Martin Lake, Saskatchewan. *Can. Mineral.* **10**, 207-215.

Harris, D.C., Cabri, J. & Murray, E.J. (1970): An occurrence of sulphur-bearing berzelianite. *Can. Mineral.* **10**, 737-740.

Hatert, F. (2005): Transformation sequences of copper sulfides at Vielsalm, Stavelot Massif, Belgium. *Can. Mineral.* **43**, 623-635.

Jedwab, J., Cassedanne, J.P., Criddle, A.J., Ry, P. (du), Ghysens, G., Meisser, N., Piret, P. & Stanley, C.J. (1993): Rediscovery of palladinite PdO from Itabira (Minas Gerais, Brazil) and from Ruwe (Shaba, Zaire). *Terra Abstracts, Suppl. to Terra Nova* **5**, 22.

Jedwab, J. (1997): Minéralogie des métaux du groupe du platine au Shaba, Zaïre. *In* Gisements de Cuivre Stratiformes

et Minéralisations Associées (J.-M. Charlet, ed.). *Mém. Acad. Roy. Sci. Outre-Mer*, 325-355.

JOHAN, Z., PICOT, P., PIERROT, R. & VERBEEK, T. (1970): L'oosterboschite $(Pd,Cu)_7Se_5$, une nouvelle espèce minérale et la trogtalite cupro-palladifère de Musonoï (Katanga). *Bull. Soc. fr. Minéral. Cristallogr.* **93**, 476-481.

LAMBERT, I., MCKAY, A. & MIEZITIS, Y. (2001): Australia's uranium resources and production in a world context. ANA Conf., Canberra, Australia.

MOH, G.H. (1964): Blaubleibender Covellite. *Carnegie Inst. Wash., Yearbook* **63**, 288.

MORIMOTO, N. & KULLERUD, G. (1963): Polymorphism in digenite. *Am. Mineral.* **48**, 110-123.

NUFFIELD, E.W. (1966): *X-Ray Diffraction Methods*. John Wiley & Sons Inc., New York, N.Y.

OOSTERBOSCH, R., PICOT, P. & PIERROT, R. (1964): La digénite sélénifère de Musonoï (Katanga). *Bull. Soc. fr. Minéral. Cristallogr.* **87**, 613-617.

PICOT, P. & JOHAN, Z. (1982): Atlas des minéraux métalliques. *Bur. Rech. Géol. Minières, Mém.* **90**.

PIERROT, R., TOUSSAINT, J. & VERBEEK, T. (1965): La guilleminite, une nouvelle espèce minérale. *Bull. Soc. fr. Minéral. Cristallogr.* **88**, 132-135.

PIRARD, C. (2005): *Etude de la minéralisation Cu–U–Se de la mine de Musonoï, Kolwezi, Katanga, RDC*. Thèse de diplôme, Université de Liège, Liège, Belgique.

POTTER, R.W. (1977): An electrochemical investigation of the system copper–sulphur. *Econ. Geol.* **72**, 1524-1542.

ROBERTS, A.C., PAAR, W.H., COOPER, M.A., TOPA, D., CRIDDLE, A.J. & JEDWAB, J. (2002): Verbeekite, monoclinic $PdSe_2$, a new mineral from the Musonoi Cu–Co–Mn–U mine, near Kolwezi, Shaba Province, Democratic Republic of Congo. *Mineral. Mag.* **66**, 173-179.

WHITESIDE, L.S. & GOBLE, R.J. (1986): Structural and compositional changes in copper sulfides during leaching and dissolution. *Can. Mineral.* **24**, 247-258.

YAMAMOTO, K. & KASHIDA, S. (1991): X-ray study of the average structure of Cu_2Se and $Cu_{1.8}Se$ in the room temperature and the high temperature phases. *J. Solid State Chem.* **93**, 202-211.

ZEN, E-AN (1956): Validity of "Vegard's Law". *Am. Mineral.* **41**, 523-524.

Received January 17, 2007, revised manuscript accepted December 30, 2007.